

# Stripes and spin-incommensurabilities are favored by lattice anisotropies

Federico Becca,<sup>1</sup> Luca Capriotti,<sup>2</sup> and Sandro Sorella<sup>3</sup>

<sup>1</sup> *Institut de Physique Théorique, Université de Lausanne, CH-1015 Lausanne, Switzerland*

<sup>2</sup> *Istituto Nazionale per la Fisica della Materia, Unità di Firenze, I-50125 Firenze, Italy*

<sup>3</sup> *Istituto Nazionale per la Fisica della Materia and International School for Advanced Studies, 34013 Trieste, Italy*

(November 1, 2018)

Structural distortions in cuprate materials give a natural origin for anisotropies in electron properties. We study a modified one-band  $t$ - $J$  model in which we allow for different hoppings and antiferromagnetic couplings in the two spatial directions ( $t_x \neq t_y$  and  $J_x \neq J_y$ ). Incommensurate peaks in the spin structure factor show up only in the presence of a lattice anisotropy, whereas charge correlations, indicating enhanced fluctuations at incommensurate wave vectors, are almost unaffected with respect to the isotropic case.

74.20.Mn, 71.10.Fd, 71.10.Pm, 71.27.+a

The experimental finding of electron inhomogeneities, the so-called stripes, in doped Mott insulators has recently stimulated a great debate. The first experimental detection of stripes in a family of  $\text{La}_{2-x}\text{Sr}_x\text{CuO}_4$  (LSCO) cuprates was achieved in a Neodymium co-doped compound,  $\text{La}_{1.6-x}\text{Nd}_{0.4}\text{Sr}_x\text{CuO}_4$ . By using neutron diffraction measurements, Tranquada and co-workers, [1,2] found that the magnetic peak at  $Q = (\pi, \pi)$  splits by a quantity  $x$ , giving rise to four incommensurate peaks around  $Q$ . Moreover, the Bragg peaks split by  $2x$  around the  $\Gamma$  point. This fact has been interpreted with the formation of charge domain walls separated by antiferromagnetic regions where no holes are present. Moreover, the incommensurate magnetic peak reveals a  $\pi$ -phase shift of the staggered magnetization when crossing the domain walls. Further studies [3] show that similar low-energy magnetic peaks occur also in  $\text{YBa}_2\text{Cu}_3\text{O}_{6.6}$ , indicating that the incommensurate spin peaks are common features of all cuprates. The Nd-doping on LSCO produces a structural transition of the  $\text{CuO}_2$  plane from the low-temperature orthorhombic (LTO) to the low-temperature tetragonal (LTT) phase. [4] In the LTO phase the Oxygen atoms are displaced out the Copper plane and there is only one Cu–O bond length, see Fig. 1(a). In the LTT phase, instead, the Cu–O bonds are not equivalent in the two directions. In one direction the Oxygen atoms are precisely in the Copper plane, while in the other the Oxygens are displaced out of the Copper plane, see Fig. 1(b). The Cu–Cu hopping depends on the Cu–O bond and it is isotropic in the LTO phase and anisotropic in the LTT one.

In this letter, we show that the anisotropies in the  $\text{CuO}_2$  may help in determining incommensurate electron correlations. [5,6] In particular, the anisotropy in the antiferromagnetic coupling favors huge incommensurate spin peaks. These peaks, although reduced, persist also when considering the anisotropy in the hopping, indicating that the structural transition may be responsible for the electron incommensurability, even if other physical effects may cooperate in the occurrence of the striped

phase. The fact that no sign of enhanced charge fluctuations are detected in the presence of spatial anisotropies does not contradict the experimental finding, which are sensible to the spin degrees of freedom and not to the electronic charge. Finally, we show that the superconducting pairing is suppressed only along the stripe, supporting a coexistence of incommensurate spin fluctuations and superconductivity, as found in Ref. [2].

We consider a two-dimensional  $t$ - $J$  model with different coupling in the  $x$  and  $y$  directions:

$$\mathcal{H} = \sum_{i,\mu=x,y} J_\mu \left( \mathbf{S}_i \cdot \mathbf{S}_{i+\mu} - \frac{1}{4} n_i n_{i+\mu} \right) - \sum_{\sigma,i,\mu=x,y} t_\mu \tilde{c}_{i,\sigma}^\dagger \tilde{c}_{i+\mu,\sigma} + H.c., \quad (1)$$

where  $\tilde{c}_{i,\sigma}^\dagger = c_{i,\sigma}^\dagger (1 - n_{i,\bar{\sigma}})$ ,  $n_i$  and  $\mathbf{S}_i$  are the electron density and spin on site  $i$ , respectively. The anisotropies are given by the fact that  $t_\mu = \alpha_\mu t$  and  $J_\mu = \beta_\mu J$ .

We use different Quantum Monte Carlo (QMC) techniques to estimate the ground-state properties of the Hamiltonian (1). In particular, we apply the recent QMC method based on the application of  $p$  Lanczos steps to a given variational wave function. [7] Moreover, we also used the fixed-node [8] and stochastic reconfiguration (SR) [7] approximations. We consider the  $p = 0$  and the  $p = 1$  state as the guiding wave function for the fixed-node method, and, hereafter, the symbols FN and FNLS indicate the fixed-node approximation with the  $p = 0$  and  $p = 1$  wave functions, respectively. Although these techniques provide a considerable improvement of the simple variational calculation, they crucially depend on the choice of the guiding wave function. Both the fixed-node and the SR are exact both in the limit of strong anisotropy ( $t_x = J_x = 0$  and any doping) and in the low-doping limit (any anisotropy) and therefore they represent reliable approximations for this problem.

The best variational wave function is the projected BCS state

$$|\Psi_G\rangle = \mathcal{P}_N \mathcal{P}_G \mathcal{J} \exp\left(\sum_{i,j} f_{i,j} c_{i,\uparrow}^\dagger c_{j,\downarrow}^\dagger\right) |0\rangle, \quad (2)$$

where  $\mathcal{P}_N$  is the projector onto the subspace of  $N$  particles,  $\mathcal{P}_G$  is the Gutzwiller projector, which forbids doubly occupied sites,  $\mathcal{J} = \exp(\sum_{i,j} v_{i,j} h_i h_j)$  is a Jastrow factor, defined in term of the hole density at site  $i$   $h_i = (1 - n_{i\uparrow})(1 - n_{i\downarrow})$ , and  $v_{i,j}$  are variational parameters. The variational parameters  $f_{i,j}$  represent the pair amplitude of the BCS wave function.

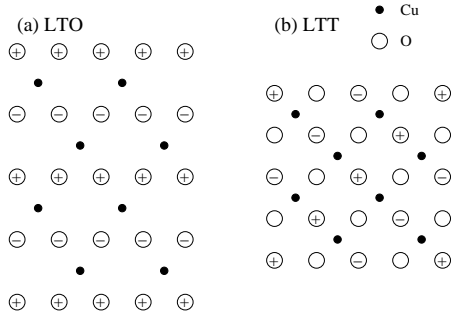


FIG. 1. A schematic representation of the  $\text{CuO}_2$  plane in the LTO (a) and in the LTT (b) lattice structure. The black circles represent Coppers, which are in the plane in both structures. Large circles represent Oxygens, the symbol + (−) indicates that the atom is shifted above (below) the Copper plane.

The wave function (2) naturally describes a Resonating Valence Bond (RVB) state in which preformed pairs become superconducting by doping. [9,10] Whenever the lattice does not break any translational and rotational symmetries and  $J \lesssim 0.5t$ , the wave function (2) is an exceptionally good approximation of the ground state of the  $t-J$  model. [7] For instance, in the case of 4 holes on a 26 lattice and  $J = 0.5t$ , the overlap of this wave function with the exact ground state is 0.88. In the isotropic model, by using QMC and starting from this very accurate wave function, it is then possible to obtain almost exact ground-state properties also for large lattices, indicating a small but finite superconducting order parameter and no charge inhomogeneities. [11] On the other hand, density matrix renormalization group (DMRG) calculations for  $J \lesssim 0.5t$  are interpreted as a strong tendency of the ground state toward the formation of static stripes. [12] These results, however, were obtained for rectangular clusters and a particular choice of the boundary conditions: periodic (open) along the short (long) direction. The first choice breaks the rotational symmetry, the second one breaks also the translational invariance.

In order to understand how stripes are stabilized, it is important to release in the model only the rotational invariance, without spoiling the translational symmetry. In fact the LTO  $\rightarrow$  LTT transition leads to a conformation which naturally breaks the rotational invariance, preserv-

ing the translational symmetry of the underlying lattice. We begin by considering a rectangular lattice  $4 \times 8$  with periodic boundary conditions (PBC) on both directions and 4 holes, for the case with no anisotropy in the couplings,  $\alpha_\mu = \beta_\mu = 1$  and  $J = 0.4t$ . In Fig. 2(a,b), we report the density-density correlations  $N(q) = \langle n_q n_{-q} \rangle$  for the variational wave function with  $p = 0$ , for the FN, FNLS and SR approximations. In this case the variational state does not present any particular structure in the density correlations, and the  $p = 1$  and 2 results do not change the overall nature of the state. Instead, the more involved FN, FNLS and SR approaches give rise to a huge peak at  $q_c = (0, \pi/2)$ . The FN, FNLS and SR methods are able to detect the right tendency of the charge arrangement, because the approximate ground state sampled by these techniques can allow the formation of many-holes bound states, not present in the wave function (2), containing only two-body correlations.

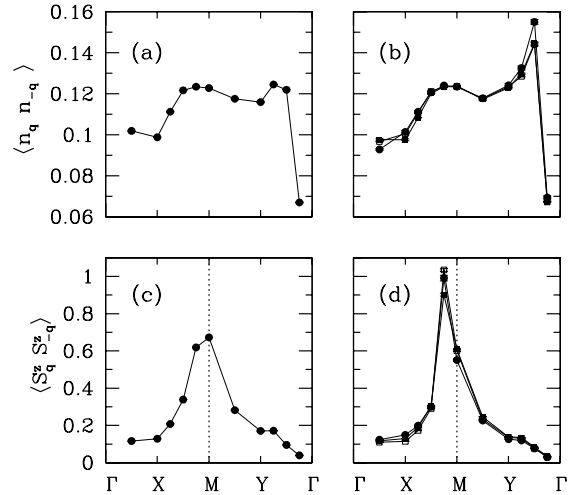


FIG. 2.  $N(q)$  and  $S(q)$  for 4 holes on a  $4 \times 8$  lattice and  $J = 0.4t$ . (a) Variational with  $p = 0$ , (b) FN (empty squares), FNLS (full squares) and SR (full circles) results for  $N(q)$ . (c) Variational with  $p = 0$ , (d) FN (empty squares), FNLS (full squares) and SR (full circles) results for  $S(q)$ .  $\Gamma = (0, 0)$ ,  $M = (\pi, \pi)$ ,  $X = (\pi, 0)$ ,  $Y = (0, \pi)$ .

From the experimental point of view, the most important signature of stripes is the appearance of well-defined incommensurate peaks in the magnetic structure factor  $S(q, \omega)$  at small energies. It is really impressive that, by using the FN, FNLS and SR approaches, we find the same fingerprint of stripes in the equal-time correlations  $S(q) = \langle S_q^z S_{-q}^z \rangle$ , as reported in Fig. 2(c,d). For the most accurate calculations, the  $Q$ -peak splits into two peaks at  $q_s = (\pi, \pi \pm \pi/4)$ , indicating that the modulation in the spins is twice the one in the charge. [13]

This calculation clearly shows that stripes can be derived by weak perturbations over the state of Eq. (2): many pairs may bound together along a preferred direction, and are stabilized in the  $t-J$  model, if the rotational

symmetry of the  $\text{CuO}_2$  plane is explicitly broken.

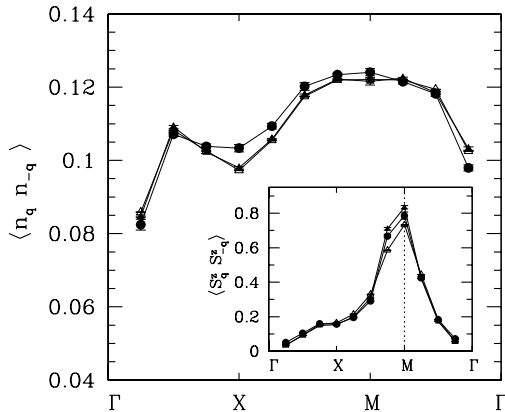


FIG. 3.  $N(q)$  for 8 holes on a  $8 \times 8$  isotropic lattice and  $J = 0.4t$ . Variational with  $p = 0$  (empty triangles), FN (full triangles) and SR (full circles) results are reported. In the inset: the same for  $S(q)$ .

In the following we compare square lattices with PBC on both directions with and without anisotropies. In the latter case, for moderate hole doping  $\delta \sim 0.1$  and  $J \sim 0.5t$ , the wave function (2) is an accurate approximation of the ground state: as shown in Fig. 3 there are no changes in the correlation functions by improving the approximation used. As emphasized in Figs. 2 and 3, within our approach, there is a strong influence of the boundary conditions for the stabilization of stripes. Within the DMRG, it was not possible to realize the important role played by the boundary conditions. Indeed, it is well known that DMRG calculations are not accurate for PBC, especially on two-dimensional clusters, where it is not possible to reproduce the homogeneous ground state even on the  $6 \times 6$ . Although for few chains our approach is less accurate – but qualitatively correct – than DMRG, [14] it is more suitable for two-dimensional lattices. The fact that QMC is competitive with DMRG is confirmed by the fact that on an  $8 \times 8$  lattice with open boundary conditions (OBC) on both directions (where the DMRG is much more accurate than PBC),  $J = 0.4t$  and 8 holes, the SR variational energy,  $E = -39.296(6)t$ , is lower than a “state of the art” (4200 states kept) DMRG calculation,  $E = -39.2503t$ , and very close to the extrapolated result, consistent for both techniques,  $E = -39.44(4)t$ . [15]

The presence of anisotropies strongly affects the outcome given by Fig. 3. Indeed, by comparing Fig. 4 with the analogous one without anisotropy (Fig. 3), it appears that the spin-spin correlations are strongly affected by the anisotropy: though at the pure  $p = 0$  variational level  $S(q)$  has a broad peak around the antiferromagnetic vector  $Q$ , within the SR technique, incommensurate peaks at  $(\pi, \pi \pm \pi/4)$  show up, see Fig. 4(a,b). We expect that the exact value of these peaks is underestimated and that they are much more pronounced in the

exact ground state. Indeed, whenever the ground-state correlations are qualitatively different from the ones of the projected BCS wave function, by using the SR (or the fixed-node) approach it is possible to detect the most relevant changes in the correlations. The incommensurate peaks for 8 holes on  $8 \times 8$  and 18 holes on  $12 \times 12$  lattices are consistent with two half-filled and 3/4-filled stripes, respectively. It is worth noting that 3 half-filled stripes in the  $12 \times 12$  give rise to 3  $\pi$ -shifts which are not compatible with PBC. Thus, it is not clear at present what the is most stable stripe filling in the thermodynamical limit (from half to completely filled stripes [16]).

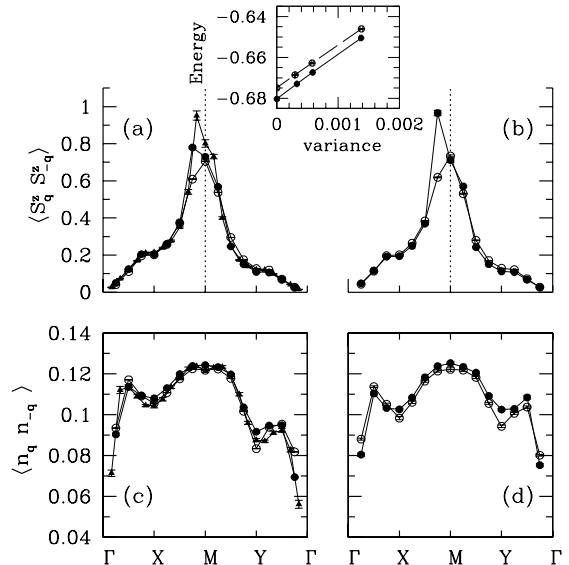


FIG. 4. (a):  $S(q)$  for  $\alpha_x = 1.1$ ,  $\alpha_y = 0.9$  and  $\beta_\mu = \alpha_\mu^2$  (case 1). Empty and full circles: variational with  $p = 0$  and SR results for 8 holes on a  $8 \times 8$  lattice. Full triangles: SR results for 18 holes on a  $12 \times 12$  lattice. (b):  $S(q)$  for 8 holes on the  $8 \times 8$  lattice with  $\alpha_\mu = 1$ ,  $\beta_x = 1.2$  and  $\beta_y = 0.8$  (case 2). (c): the same as (a) for  $N(q)$ . (d): the same as (b) for  $N(q)$ . In the inset: the energy per site extrapolation for  $p = 0, 1, 2$  Lanczos steps for the case 1 (continuous line) and for the case 2 (dashed line), for the  $8 \times 8$  lattice. The extrapolated points are also shown.

The effect of the lattice anisotropy on the charge correlations is much less evident and  $N(q)$  does not show sizable differences between different approaches, see Fig. 4(c,d). We stress that the neutron scattering is only sensible to the electronic spin and there is no direct information on electronic charge. The finite peak at small- $q$  in the  $N(q)$  may be attributed to dynamical fluctuations of the stripes, which do not affect the  $S(q)$  incommensurate peak, but destroy a coherent response in the static charge correlations. In order to have this outcome, it is important that the spins across the stripes are strongly antiferromagnetically correlated. [17] We have verified that, in the anisotropic case, the spin-spin correlation across an hole has a strong antiferromagnetic character. The above

scenario is confirmed by the fact that the anisotropy in  $t$  favors the transverse motion of the domain walls, yielding a suppression of the incommensurate peak of  $S(q)$ , as shown in Fig. 4(a,b) for the  $8 \times 8$  case. Well defined static stripes are instead defined in the system by considering OBC. As shown in Fig. 5, in the  $8 \times 8$  cluster there is a clear tendency to formation half-filled stripes, although in the variational calculation no signature of inhomogeneities is present. For 4 holes there is a single stripe at the center of the lattice, whereas for 8 holes, two of such features clearly appear, indicating the half-filled character.

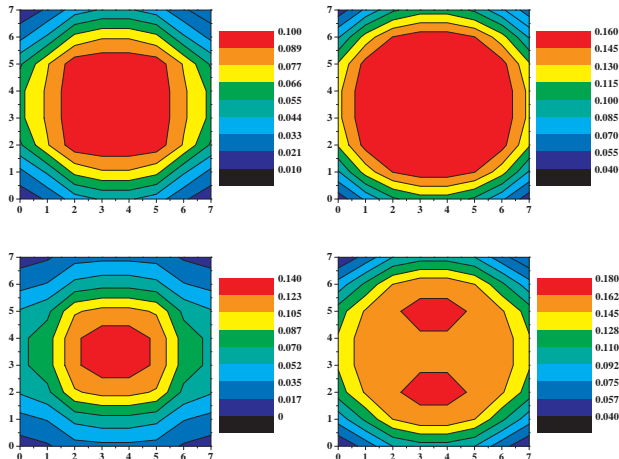


FIG. 5. On the left: average hole density profile for 4 holes in a  $8 \times 8$  lattice with OBC and  $J = 0.4t$ ,  $\alpha_\mu = 1$ ,  $\beta_x = 1.2$  and  $\beta_y = 0.8$  (case 2 of Fig. 4), for the  $p = 0$  calculation (upper-left panel) and for the SR technique (lower-left panel). On the right: the same for 8 holes.

In order to study the role of the anisotropies on the superconductivity, we consider the pair-pair correlation function  $\Delta_{i,j,k,l}$ , which creates a singlet in the sites  $i$  and  $j$  and destroys it in the sites  $k$  and  $l$ . The results are reported in Fig. 6. The effect of the anisotropy is to depress the pairing function along the stripe, whereas the pairing remains almost unchanged in the perpendicular direction. This effect is particularly strong in the  $4 \times 8$  lattice where pairing correlations are suppressed by more than an order of magnitude along the stripe.

In conclusions, in the presence of anisotropies, our finding is consistent with fluctuating stripes, where the  $\pi$ -phase shift gives rise to incommensurate peaks in the  $S(q)$  and to an almost featureless  $N(q)$ . We finally remark that stripes do not necessarily suppress superconductivity, but large pairing correlations can be obtained in the direction perpendicular to the stripes. On the other hand,  $d$ -wave superconductivity is a very robust property of an isotropic doped antiferromagnet, implying that the RVB scenario represents a reasonable explanation of high-temperature superconductivity.

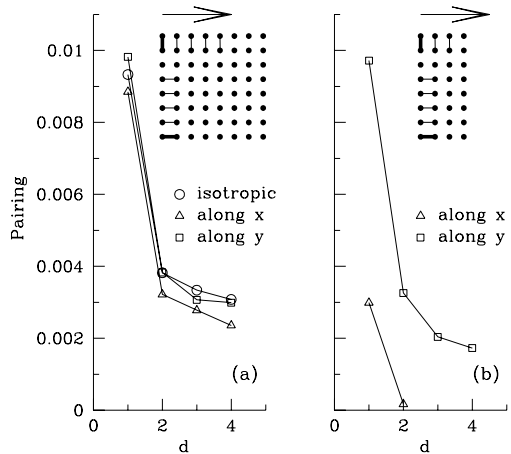


FIG. 6. (a): pairing correlation function  $\Delta_{i,j,k,l}$  obtained with SR for the isotropic  $8 \times 8$  lattice of Fig. 3 (circles) and the anisotropic one of Fig. 4(b,d) (triangles and squares). (b): the same for the  $4 \times 8$  lattice of Fig. 2. The pairs  $(k, l)$  (thin lines) are obtained by moving the pair  $(i, j)$  (thick line) parallel to the  $x$  or the  $y$  axis,  $d$  is the distance between pairs. The direction of the stripes is defined by the arrow.

We thank E. Dagotto, C. Gazza, G.B. Martins, T.M. Rice, M. Calandra, A. Parola, M. Fabrizio, A. Bianconi and C. Morais Smith for useful comments. This work has been partially supported by MURST (COFIN99).

- 
- [1] J.M. Tranquada *et al.*, Nature **375**, 561 (1995).
  - [2] J.M. Tranquada *et al.*, Phys. Rev. Lett. **78**, 338 (1997).
  - [3] H.A. Mook *et al.*, Nature **395**, 580 (1998).
  - [4] J.D. Axe *et al.*, Phys. Rev. Lett. **62**, 2751 (1989).
  - [5] B. Normand and A.P. Kampf, Phys. Rev. B **64**, 024521 (2001).
  - [6] A.P. Kampf *et al.*, Phys. Rev. B **64**, 052509 (2001).
  - [7] S. Sorella, Phys. Rev. B **64**, 024512 (2001).
  - [8] D.F.B. ten Haaf *et al.*, Phys. Rev. B **51**, 13039 (1995).
  - [9] P.W. Anderson, Science **235**, 1196 (1987).
  - [10] A. Paramekanti *et al.*, cond-mat/0101121.
  - [11] M. Calandra and S. Sorella, Phys. Rev. B **61**, 11894 (2000).
  - [12] S.R. White and D.J. Scalapino, Phys. Rev. Lett. **80**, 1272 (1998)
  - [13] C. Gazza, G.B. Martins and E. Dagotto, by using DMRG, found similar results for  $J = 0.2t$ , private communication.
  - [14] S. Sorella *et al.*, in preparation.
  - [15] S.R. White, private communication.
  - [16] S.R. White and D.J. Scalapino, Phys. Rev. Lett. **81**, 3227 (1998).
  - [17] G.B. Martins *et al.*, Phys. Rev. Lett. **84**, 5844 (2000).